IEEE Access
Multidisciplinary ⋮ Rapid Review ⋮ Open Access Journal

Received July 22, 2021, accepted August 2, 2021, date of publication August 13, 2021, date of current version August 27, 2021.

Digital Object Identifier 10.1109/ACCESS.2021.3104729

Renewable Wave Energy Potential for the Sustainable Offshore Oil Platforms in South China Sea

ZAFARULLAH NIZAMANI[1], LEE LI NA[1], AKIHIKO NAKAYAMA[1], MONTASIR OSMAN AHMED ALI[2], AND MUSHTAQ AHMED NIZAMANI[1]

[1]Department of Environmental Engineering, Universiti Tunku Abdul Rahman, Kampar, Perak 31900, Malaysia
[2]Department of Civil and Environmental Engineering, Universiti Teknologi PETRONAS, Seri Iskandar, Perak 32610, Malaysia

Corresponding author: Zafarullah Nizamani (zafarullah@utar.edu.my)

This work was supported by the Ministry of Higher Education, Malaysia, through the research fund, Fundamental Research Grant Scheme under Grant FRGS /1/2018/TK01/UTAR/02/4.

ABSTRACT The Jacket platform needs gas and diesel to run its turbines, and in the end, they produce catastrophic emissions annually. The environmental concerns regarding these platforms have forced us to utilize an alternative source of energy that is sustainable and clean. In this study 51 locations, are of interest where oil and gas activities are in progress at present in the shape of a jacket platform or pipelines. The significant wave height and wave period scatter diagram data are collected from the platforms in the South China Sea. The linear wave theory is used to find the wave power. The given time period is converted into an equivalent time period first before wave energy is determined. The study shows that location no. 20 is the ideal location to deploy the wave energy converter Pelamis P2 with a potential mean wave power of 6.61 kW/m A single unit of Pelamis P2 can produce on an average electricity output of 91.37 kW/m including, the losses and machine efficiencies, whereas a wave farm can generate an average output of 62 GWh/ yr. The electricity supply of 70.3 % of the minimum and 14.1 % of the maximum energy demand, while using only wave energy converter. If hybrid wind and wave energy system is used, then energy production will increase. The results show that the wave farm could also reduce the use of natural gas up to 17.6E06 m^3/ year, avoiding the emission of 12000 tonnes of CO and 54000 tonnes of NOx annually, and can save up to RM 20 billion annually with the reduction of natural gas emissions.

INDEX TERMS Wave energy converter, renewable energy, South China Sea, metocean, jacket platform.

I. INTRODUCTION

Fixed and floating platforms are most suitable to extract fossil fuels in offshore Malaysia near the continental shelf of the South China Sea (SCS). Coal, oil, and natural gas are used as fossil fuels to meet today's energy demand. Malaysia relies on natural resources such as oil, natural gas, which it produces locally, to achieve its energy demand. Most of its reservoir resources are drilled in the South China Sea (SCS) using jacket platforms. The Oil and Gas (O&G) reserves in offshore Malaysia are in three regions Peninsular Malaysia (PMO), Sarawak (SKO), and Sabah (SBO). The offshore O&G activities require a considerable amount of energy to maintain their continuous operation and production. Moreover, the conventional means to supply the electric power for O&G activities is by using the fossil fuels such as diesel which produces high levels of carbon dioxide (CO_2), leaving a huge carbon footprint on the environment.

At present, the renewable energy source is solar, wind, and fuel cell, however, ocean waves, current, and tides can play a significant role to produce future renewable energy. Ocean renewable energy is the energy harnessed from the marine environment that causes little to no carbon footprint to the environment, Wave Energy Converters (WECs) are used to generate it. To reduce the carbon footprint from the industry and using wave energy as an alternative energy supply for offshore O&G activity is a significant step that can be taken by the government. The idea of integrating renewable wave energy systems to the offshore oil platforms can reduce the environmental impact of the platforms. In addition to

The associate editor coordinating the review of this manuscript and approving it for publication was Jing Yan.

that, it can also increase the percentage of renewable energy input for the country's clean energy production. Offshore oil operations can be separated into two main stages, upstream and downstream. The upstream activities stage involves the field exploration, development, fabrication, installation of platform, extraction, and production of raw materials from the site. The downstream process involves the refining of the raw materials into usable products and their sales and distribution [1].

The extraction of oil from the offshore field requires a large amount of energy and diesel and natural gas are used as a fuel for the turbine operation to produce energy [2]. Offshore platforms may also be powered by electricity from onshore grids transmitted via subsea cables. Energy generated using diesel emits a large quantity of pollutants and causes an adverse impact on the environment. In addition to that, the reduction of O&G output due to the maturity of fields reduces the sustainability of the platforms. Hence, diversifying the energy supplied for the offshore operations may improve the sustainability of the platforms.

The idea of using renewable energy sources as an alternate power source for offshore oil operations has been gaining interest in recent years [2]. However, most of the research and development is focused on mature technologies such as solar and wind energy. In addition to that, only a handful of articles that study integrating wave energy with offshore oil platforms can be found. Hence, comes the motivation to assess the feasibility of supplying offshore oil platforms with alternate off-grid energy using the wave energy systems. The potential of offshore wave power from the SCS is a new and developing field. As a case study, three regions of Malaysia from the SCS, are considered here for the feasibility of the wave energy converter and the best location for wave energy farm development. It has been assumed in many studies that it is considered that wave energy is available in the ocean when the mean wave energy flux is 1 kW/m or higher [3]. It is also considered in this study that rough and disruptive waves during high seas (typhoon and storms), can cause serious damage to the Wave Energy Converters such as Significant wave height is greater than 4.0 [4].

A. RENEWABLE ENERGY

According to the International Energy Agency (IEA), the capacity of global oceans is about 93,100 TWh/year. One of the Sustainable Development Goals (SDGs) of the United Nations (UN) is to ensure access to clean and renewable energy that is cheap, reliable, and sustainable [5]. To achieve this goal Malaysian government in its eleventh five-year Plan (2016-2020) introduced to ensure the development of reliable and affordable energy and reduce the country's reliance on non-renewable fossil fuels [6]. In 2018, Malaysia had set its target to have renewable energy sources (RESs) contributing 20% of the country's electricity by 2025 [7]. The generation of energy from fossil fuels is cheap however it brings an adverse impact on the people, environment as well as economy. Kyoto Protocol indicating global warming had aroused significant attention in the generation of renewable ocean energy.

During energy generation, the combustion of fossil fuel produces a large amount of greenhouse gases, i.e., carbon dioxide (CO2), carbon monoxide (CO), methane (CH4), nitrogen oxides (NOx). The CO2 increases the environment's temperature, leading to global warming. Studies have revealed that electricity and heat generation produce the most CO2 in the European Union (EU) [8]. The International Energy Agency (IEA) compared the global energy demand and global CO2 emission between the first quarter (Q1) of the year 2019 and the first quarter of 2020. It is reported that the global energy demand from coal and oil in Q1 of 2020 has declined as compared to Q1 of 2019 due to the restricted movement and economic activity during the coronavirus pandemic [10]. Moreover, the decline of global demand for coal and oil was the major contributor to the decline in global emissions detected in Q1 of 2020. This shows that by reducing the use of fossil fuels, the CO_2 in the environment can be greatly reduced.

Energy security can be defined as energy that is available at unchanging prices without the risk of discontinuation [11]. With the diminishing quantity of fossil fuels and increasing energy demand, the competition over the resources will increase and can cause instability in the pricing of the energy. The current O&G reserves of Malaysia are expected to last until 2035 [12] and this will lead to energy insecurity in Malaysia. Many other countries that rely heavily on energy imports such as China, which is heavily dependent on the Persian Gulf and Africa for its oil and gas imports, with the oil import accounting for about 59 % of the country's total consumption [13], may also have to switch over to renewable energy sources in future. While in India, it is estimated that from 2018 to 2019, its oil import made up approximately 80% of the country's consumption [14]. In 2018, more than half of the EU energy demand (58.2%) depended on oil and gas imports, mainly from Russia [15].

The price of fossil fuels may also fluctuate due to economic and political reasons. A disruption of gas imports to the European market occurred when a Russia-Ukraine gas dispute broke out in 2006 and 2009, resulting in a serious effect on the economy and society [16]. In contrast, under optimal conditions, the supply from renewable energy sources would never run out. Moreover, the cost of harvesting energy from renewable energy sources mainly comes from the initial capital investment to build the infrastructure and systems. Renewable energy sources are inexhaustible and do not depend on political and economic status for their stability in pricing. This is different from the non-renewables which fluctuate according to the availability of reserves [17]. While one may argue that a high price is required for investing the capital expenditure for the harvesting and utilization of renewable energy, advancing technology and improvements in its further development may eventually cause a reduction in the pricing of renewable energy sources such as solar and wind power. For example, the price of electricity generated using

solar photovoltaic (SPV) was observed to have dropped, from $300 per watt in 1954 to $4.5 per watt in 2007 [18]. Renewable energy sources are domestic, by transitioning from conventional fossil fuels to renewable energy sources, the dependence on energy imports can be reduced, allowing the country to be self-sufficient. Not much work has been done on the wave energy resources around Malaysia remains scarcely published and offshore wave power densities need to be evaluated. The wave energy resources surrounding Malaysia are not well studied and this area is still afresh in terms of a major contribution.

B. ENERGY DEMAND FOR AN OFFSHORE OIL PLATFORMS

The energy demand for each platform varies due to its size and well capacity. Tiong, *et al.*, used a platform in their study with energy demand in the range of 10-50 MW [19], where the specific platform analysed has a demand of 10 MW on a SHELL Malaysia Oil and Gas Platform in Sabah. Ardal, *et al.*, has mentioned the power demand in the range of 40-45 MW [20]. Zhang, *et al.*, studied four offshore platforms, each with different activities (extraction, processing, support and maintenance, and storage) gives a peak power demand of approximately 44 MW [21]. Another difference is that the platforms may operate individually or work together to form a single and central power platform, providing power to the others. Korpas *et al.* stated that the power consumption by the oil platform studied is about 20 MW to 35 MW [22]. Nguyen, *et al.*, state that the power demands of four platforms (named Platform A, B, C, and D) located in Norway range from 5.5 MW to 30 MW [9]. The variation in values most likely is because of the different products generated on each platform, involving different processes and operations for each platform. In addition to that, the demand for heating can also be fulfilled with a range of 1 MW to 12 MW [9].

The platforms use either natural gas or diesel but sometimes both can be used alternatively as a fuel to generate electricity. Oliveira-Pinto, *et al.* state that, 50 % of the energy supply was to be fulfilled by natural gas while diesel fuels supply the other 50 % [2]. On the other hand, Zhang, *et al.* found co-firing turbines at the platforms which can run on natural gas, diesel, or hydrogen [21]. The energy demand for some of the offshore oil platforms is shown in Table 1, where the energy requirements vary from 10 MW to 45 MW depending on the well sizes.

This study will use the energy demand in a range of 10-50 MW as the minimum and maximum requirement of energy supply and assesses the wave energy resources at locations active with O&G activities in the offshore region of Malaysia, SCS. The electricity generated by WECs is estimated and taken into consideration in deciding the best-suited location for offshore wave energy development. The feasibility of the energy project is also assessed and evaluated to determine if it can meet the energy demand required by the offshore oil platforms.

II. WAVE ENERGY CONVERTERS (WECS)

The process of Wave energy converters is based on forces induced by the ocean waves that produce relative motion between various parts of the converter system. Mechanical or electrodynamic systems are used to generate energy. The energy will not be produced if the WEC device is moving up and down at the free surface of the ocean. The device needs to be attached to form a lever that will allow the wave energy conversion into a new form of energy. The lever is attached to a dashpot to convert the mechanical energy into heat [4]. Wave energy converters (WECs) harness the energy from the ocean, converting wave energy into electricity [23]. A WEC mainly consists of a hydrodynamic subsystem that captures the wave energy, a power take-off (PTO) that converts energy into electricity, a reaction subsystem to hold the WEC in position, and a control subsystem that controls and monitors the subsystem [23].

Early wave devices are considered a modest wave resource at the coastline. There are some advantages for the coastal locations as compared to the deep water. (a) WEC can be easily installed; thus commissioning costs will be reduced. (b) WEC is rigidly fixed to the sea bed and thus providing more robust opportunities for extraction of energy. (c) Electricity distribution costs will be reduced due to the expensive sea-bed power cables. (d) Maintenance costs will be lesser because of greater accessibility [4]. Due to its wide variety, WECs can be categorized into different ways. One of the ways is to categorize them based on the location where the device will be installed, whether onshore, nearshore or offshore. The nearshore devices, usually mounted at the seabed, are located at water depths where seabed will influence the waves; offshore devices, usually floating at the surface, are located at water depths where the waves will not be affected by the seabed [23]. Offshore offers the most energy among the three locations as no energy is lost due to the friction between the ocean waves and seabed [24]. However, at the same time, it also implies that offshore devices must withstand high loading and extreme weather conditions [25]. The categorization of WECs can also be done according to their mechanism (hydrodynamic subsystem), as oscillating water columns (OWCs), wave activated bodies, or overtopping devices [26]. Fig. 1 illustrates the principle of each category of WEC. OWCs utilize columns of water in which the movement of the ocean in the column causes wave activated bodies, known as oscillating bodies, to harvest wave energy from the ocean directly by the motion of the device itself [24]. The category of wave activated bodies can be further broken down into the point absorbers [24]. Overtopping devices involve a ramp to raise the water level of the incident waves so that the water will overflow into a reservoir [24]. As the water exits the reservoir, it turns the turbine and generates electricity [24].

There are different kinds of WECs designed to harvest wave energy in different locations as well as wave climates. Table 2 shows the Wave Dragon WEC based on the wave

TABLE 1. Energy demand of typical offshore platforms.

Year	Energy demand (MW)	Heat demand (MW)	Fuel type	Fuel capacity (MW)	Remarks	References
2014	40-45	-	Natural gas	40	Norway	[20]
2015	10	-	-	-	SHELL, Sabah Malaysia Oil and Gas Platform	[19]
2019	27		Natural gas (50%) and diesel (50 %)	39	Norway Energy supplied by four turbines, two runs on full load while the other runs on half load as backup.	[2]
2019	44	12	Natural gas or diesel	-	China Gas/oil turbines utilize diesel, natural gas, or hydrogen as fuel.	[21]
2012	20-35		Natural gas	46	North Sea	[22]
2016	A: 25 B: 5.5 C: 30 D: 19	A: 1 B: >0 C: 10 D: 5	-	-	Norway A: Oil production B: Produces gas and condensates C: Heavy oil and gas production D: Produces volatile oil and gas	[9]

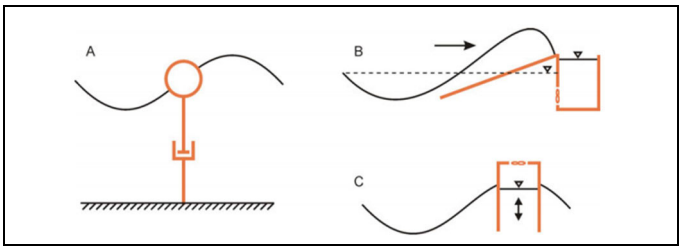

FIGURE 1. Mechanism of WECs A) wave activated bodies, B) overtopping devices (B) and C) Oscillating water columns [24].

climate of the location and energy production requirements. Fig. 2 shows two separate designs of the Wave Dragon WEC based on the wave climate. From Fig. 2, it can be observed that the wave climate affects the dimension, which in turn affects the weight and volume of the reservoir, number of turbines required for the WEC. This would then eventually impact the rated power and power production of the WEC. It can also be observed that the wave climate affects the dimension, which in turn affects the weight and volume of the reservoir, number of turbines required for the WEC. This would eventually impact the rated power and its production by the WEC.

TABLE 2. The design of wave dragon WEC according to the wave climate of the location [27].

Unit size	Prototype	24 kW/m	36 kW/m	48 kW/m	60 kW/m
Width (m) (between reflector tips)	57	260	300	390	390
Weight incl. ballast, t	237	22,000	33,000	54,000	54,000
Reservoir, m^3	55	5,000	8,000	14,000	14,000
Number of turbines	1+3+6	16	16-20	16-20	16-24
Annual power production, GWh/year	0.06	12	20	35	43
Generators (PMOG), kW	2.5	250	350-450	460-700	625-940

A. PELAMIS (P2)

The Pelamis is a semi-submerged WEC with four segments that move perpendicular to the wave motion. Thus, the Pelamis is considered as a wave activated body WEC. It utilizes a hydraulic power take-off (PTO) in which the hydraulic motor drains the oil pumped in due to the motion of WEC, driving the generator to generate electricity [26]. Fig. 2(a) shows the working principle of the Pelamis. The prototype was first tested in 2004 with its success leading to the development of the first commercial wave farm, Agucadoura in 2005 on the northern Portugal coast [29]. The first stage of the system was completed in 2006, consisting of three of the first generation Pelamis P1 [29]. A facility to be powered by the second generation Pelamis P2 was developed and tested in Scotland [29]. Thomson, *et al.* conducted a

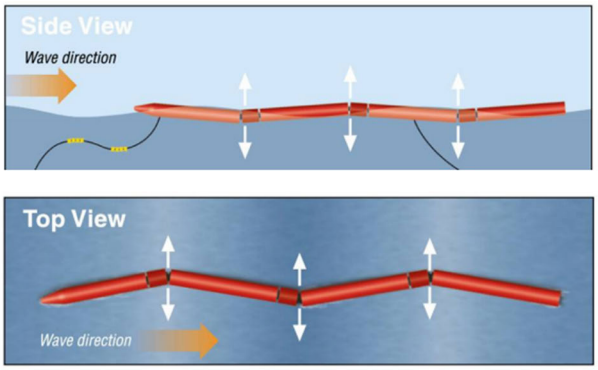

a) Working mechanism of the Pelamis [29].

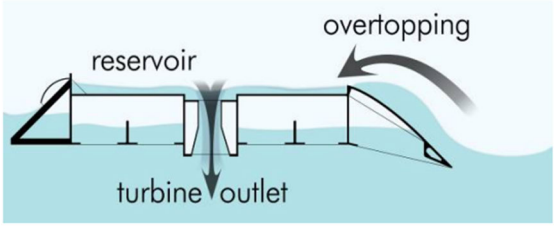

b) Working principle of the wave dragon. [30]

FIGURE 2. Types of Wave Energy Converters.

life cycle assessment (LCA) to evaluate the environmental impacts of the first-generation Pelamis P1, involving the device, mooring, and sub-sea cables connecting to the grid, and throughout its life cycle [28].

B. WAVE DRAGON

Fig. 2(b) shows the working principle of the wave dragon. The Wave Dragon is an overtopping device and had a prototype, a 20 kW being tested offshore of Denmark [30]. The WEC works by having water overtopping its ramp and overflows into the reservoir and as it leaves through the outlet, it turns the turbine hence producing power [30].

C. AQUABUOY

AquaBuoy is a small sized WEC developed by Finavera Renewables to harvest offshore wave energy. The AquaBuoy was designed based on a heaving buoy concept [32]. The WEC consists of a buoy connected to a long tube at the bottom which is known as the acceleration tube [30]. On the surface of the ocean, the buoy moves up and down as the wave passes. The kinetic energy of the waves pressurizes the fluid contained inside the tube, causing the pumped fluid to drive a turbine generator. A full-scale prototype of the AquaBuoy, was tested at a demonstration 1MW power plant offshore of Makah Bay, Washington [29]. The project involved four units of 250 kW power rated AquaBuoy and was located 5.9 km offshore at depths reaching to 46m deep.

D. ASSESSMENT OF POTENTIAL WAVE POWER

The wave power is the product of average energy density and group velocity. The wave power and group velocity of the wave are expressed as in (1)-(2) respectively [34].

$$P = Exc_g \tag{1}$$

P = Wave power (kW/m), E = Energy density (kJ), and c_g = Wave group velocity (m/s)

$$c_g = \frac{gT_e}{4\pi} \tag{2}$$

g = Gravitational acceleration, 9.81 (m/s^2), and T_e = Wave energy period (s)

Samrat, *et al.* [35] conducted an assessment for estimating the wave energy available around Malaysia using (3). Nasir and Maulud [36] calculated the potential wave power offshore of Malaysia, in terms of kilowatt per meter length of wave crest (kW/m), using (4). Equation (3) estimates the wave power by approximating waves to harmonic waves while (4) made considerations for the real ocean waves. The power density, P (W/m), is determined across a plane perpendicular to the direction of wave propagation.

$$P = \frac{\rho g^2}{32\pi} H^2 T_e \tag{3}$$

ρ = Seawater density (1.025 g/cm^3), H = Maximum wave height (2x H_S) (m). H_S = Significant wave height (m)

$$P = \frac{\rho g^2}{64\pi} H_S^2 T_e \tag{4}$$

For real ocean waves, the energy density is said to be half of the harmonic wave [24], which is expressed in (5)-(6). [24] noted that the comparison of harmonic wave H should not be made directly with the H_S. waves moving towards nearshore experience numerous form transformations i.e., shoaling, refraction, diffraction, and reflection. The offshore wave power is not affected by refraction and shoaling and is computed directly from wave data using the following deep water expression. Linear theory of water waves was originally developed by Airy. This also allows the determination of wave energy density or specific energy, E (J/m^2) i.e., energy per unit area, for a regular wave of height H (m). Equation (5) gives the energy density of harmonic waves and (6) gives the energy density of real ocean waves. To account for the real ocean waves at deep water (d > 0.5 L), (4), will eventually result in (6) which should be used instead of (3).

$$E = \frac{1}{8}\rho g H^2 \tag{5}$$

$$E = \frac{1}{16}\rho g H_S^2 \tag{6}$$

The power available in waves was calculated as given in (7) by Ciang, *et al.*, by using the average wave height and period obtained from the Malaysian Meteorological Service (MMS) are assumed to be equivalent to the HS and Te respectively [37]. Equation (7) was used to determine wave power potential at Lakshadweep, Andaman, and the Nicobar Islands was determined [38]. The energy period Te is seldom specified and must be determined from another measured period. The measured sea states are generally specified in

terms of the peak period TP or Zero Crossing Period. The relation between T_Z and T_e depends on the shape of the wave spectrum and can be expressed as $Te = \lambda T_Z$ where the λ is a coefficient that depends on the shape of the wave spectrum [39]. T_z is used in the computations instead of T_e in Eq. (7) which is formed from (4) after converting Te into Tz. For instance, in the Handbook of Ocean Wave Energy, the relation $1.12T_e = 1.29T_z = T_p$ was given for a JONSWAP wave spectrum [21]. Sharkey gave the relationship of $T_e = 1.12T_z$ [40].

$$P = 0.55 x H_S^2 x T_z \tag{7}$$

T_z = Zero-crossing period (s). Equation (6) measures the instantaneous wave power at a specific H_S and Te (or Tz). To measure the wave resource of a particular location, the mean values of the wave power, with consideration of the annual sea states, should be calculated by (9),

$$P = \frac{\rho g^2}{64\pi} \sum_{i=1}^{n_T} \sum_{j=1}^{n_{H_S}} H_{S_{ij}}^2 T_{ij} f_{ij} \tag{8}$$

$H_{S_{ij}}$ = Significant wave height corresponding to the bin at the ith line and jth column of the scatter plot (m), T_{ij} = Wave period corresponding to the bin at the ith line and jth column of the scatter plot (s), f_{ij} = Occurrence frequency corresponding to the bin at the ith line and jth column of the scatter plot [2].

III. WAVE DATA ANALYSIS AND STUDY AREA

The South China Sea has great potential for the utilization of ocean renewable energy as it is also exposed to the annual events of two seasonal monsoons. The offshore wave energy is analysed either by hindcast wave data or by metocean data and in this study data from later sources is used. The selection of location is based on the metocean data from Petronas Carigali Sdn Bhd. Table 3 (A-C) shows the locations with O&G activity in the SCS near the continental shelf of Malaysia, the coordinates, and mud level depth. Location number 1-18s are from Peninsular Malaysia, 19-39 from Sarawak, and 40-51 from the Sabah region. The maximum depth of the platform is 95 m and the minimum depth is 36 m the depth is less than this is the site for the pipelines. Two assumptions are made in this study i.e., the offshore platforms have an energy demand of 10 MW - 50 MW and the platforms depend on natural gas as their sole power supply.

A. WAVE ENERGY CONVERTER (WEC) POWER

The wave power computed from (1-8) measures the potential wave energy resources in the ocean. The amount of electricity that can be produced is highly dependent on the WECs' efficiency. Silva, *et al.* measured the electricity generated by five different WECs at a specific location by associating the power matrices of the WECs with the wave activity of that

Descriptive Statistics

Statistic	Value
Sample Size	58439
Range	4.5
Mean	1.2919
Variance	0.36725
Std. Deviation	0.60601
Coef. of Variation	0.46909
Std. Error	0.00251
Skewness	1.4992
Excess Kurtosis	2.6795

Percentile	Value
Min	0.5
5%	0.5
10%	1
25% (Q1)	1
50% (Median)	1
75% (Q3)	1.5
90%	2
95%	2.5
Max	5

FIGURE 3. Descriptive statistics output in location 2 from PMO region.

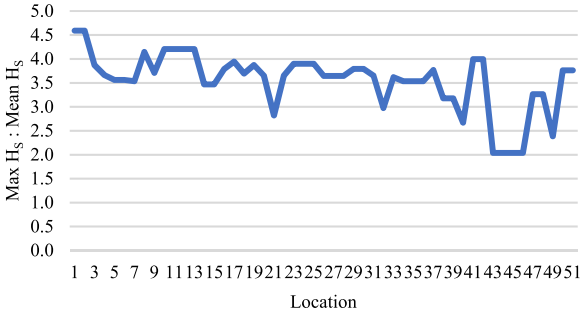

FIGURE 4. Ratio of maximum to mean H_S for all study locations.

location from the scatter plot as expressed in (10) [33].

$$P_E = \frac{1}{100} \sum_{i=1}^{n_T} \sum_{j=1}^{n_{H_S}} p_{ij} x P_{ij} \tag{9}$$

P_E = Electricity generated by WEC (kW), p_{ij} = Energy percentage corresponding to the bin at the ith line and jth column, % P_{ij} = Power corresponding to the power matrix for the WEC in consideration (kW) [33]. A variation of (10) is shown by (10) which is also used to compute the power generated by WEC. Instead of energy percentages, (10) calculates the electricity output of the WEC based on the occurrence frequency of sea states at the location [2].

$$P_E = \sum_{i=1}^{n_T} \sum_{j=1}^{n_{H_S}} f_{ij} x P_{ij} \tag{10}$$

B. MEAN WAVE POWER POTENTIAL

Using the scatter diagrams, the mean wave power potential for all locations is computed from (11).

$$P = \frac{\rho g^2}{64\pi} \sum_{i=1}^{n_T} \sum_{j=1}^{n_{H_S}} H_{S_{ij}}^2 T_{ij} f_{ij} \tag{11}$$

P = Mean wave power potential at the specific location (kW/m), H_{Sij} = Significant wave height corresponding to the bin at ith line and jth column of the scatter diagram (m), T_{ij} = Wave energy period corresponding to the bin at ith line

TABLE 3. (A) Study locations in PMO Region. (B) Study locations in SKO Region. (C) Study locations in SBO Region.

PMO	Coordinates Latitude (North, N)	Longitude (East, E)	Depth MSL (m)
1	6.1	103.3	60.7
2	6.1	105.3	60.4
3	4.8	104.9	74.7
4	5.2	104.7	75.0
5	5.2	105.5	76.3
6	5.3	105.5	74.7
7	5.4	105.2	71.4
8	7.1	103.4	60.0
9	-	-	79.2
10	6.2	104.1	76.6
11	6.3	104.0	70.0
12	5.9	104.3	63.8
13	6.0	104.2	72.2
14	5.0	105.4	75.8
15	5.0	105.3	77.0
16	5.5	105.3	65.0
17	-	-	66.4
18	6.3	103.9	60.0

(a)

SKO	Coordinates Latitude (North, N)	Longitude (East, E)	Depth MSL (m)
19	4.3	112.7	71.5
20	4.7	113.9	50.3
21	-	-	15.0
22	4.7	113.9	51.8
23	-	-	74.7
24	-	-	71.6
25	-	-	67.1
26	-	-	35.0
27	-	-	28.0
28	-	-	45.0
29	3.8	112.3	46.0
30	3.8	112.3	45.0
31	-	-	57.9
32	-	-	6.0
33	3.8	111.5	52.0
34	4.4	111.8	95.0
35	4.4	112.0	95.0
36	4.8	111.3	94.8
37	4.8	112.9	93.6
38	-	-	27.0
39	-	-	25.0

(b)

TABLE 3. *(Continued.)* (A) Study locations in PMO Region. (B) Study locations in SKO Region. (C) Study locations in SBO Region.

SBO	Coordinates Latitude (North, N)	Longitude (East, E)	Depth MSL (m)
40	5.6	114.8	57.0
41	6.5	115.7	60.0
42	6.7	115.8	60.0
43	5.6	114.9	47.0
44	5.6	115.0	52.3
45	5.6	114.9	10.0
46	5.0	114.9	11.0
47	5.0	115.0	42.8
48	5.5	115.0	36.9
49	5.6	115.0	57.4
50	5.4	114.7	59.1
51	5.4	114.7	53.1

(c)

and jth column of the scatter diagram (s), f_{ij} = Occurrence frequency corresponding to the bin at ith line, and jth column of the scatter diagram [2].

The wave powers to be computed are in terms of wave energy period, T_e, and hence, the relationship between T_E, T_z, and T_P, needs to be determined. The relationship between TE and TP is taken as $T_e = 0.9T_P$ [2]. From the metocean data, the relationship between TP and Tz is given to be $T_P = 1.41T_z$. Hence, T_z is related to T_E as $T_E = 1.27T_z$.

C. POWER OUTPUT FROM THE WAVE ENERGY CONVERTERS (WECS)

The average electric power produced by a WEC installed at a specific location can be estimated from the scatter diagram of the location and the power matrix of the WEC, from (12),

$$P_E = \sum_{i=1}^{n_T} \sum_{j=1}^{n_{H_S}} f_{ij} P_{ij} \tag{12}$$

P_E = Average electric power generated by WEC (kW), P_{ij} = Power corresponding to the power matrix for the WEC in consideration (kW), f_{ij} = Occurrence frequency of sea states in the ith line and jth column [2]. The performance of the WEC can then be measured by its capacity factor, as expressed by (13),

$$C_f = \frac{P_E}{R_p} x100 \tag{13}$$

C_f = Capacity factor of WEC (%), Rp = Rated power of WEC (kW) [2]. The capacity factor is dependent on the rated power of the WEC which varies from one WEC to another as shown in Table 4.

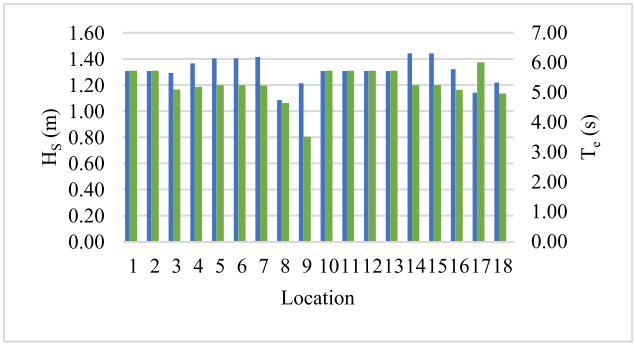

(a) Mean H_S and Mean T_e in the PMO region.

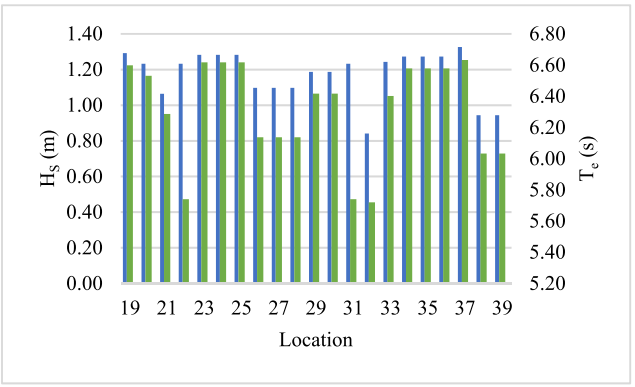

(b) Mean H_S and Mean T_e in the SKO region.

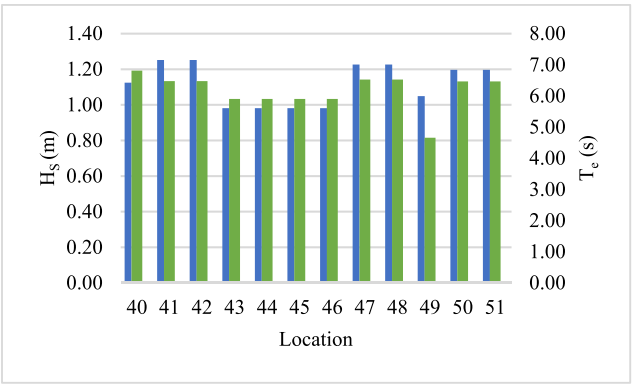

(c) Mean H_S and Mean T_e in the SBO region.

FIGURE 5. (a): Mean H_S and Mean T_e in the PMO region. (b): Mean H_S and Mean T_e in the SKO region. (c): Mean H_S and Mean T_e in the SBO region.

TABLE 4. Rated power of Pelamis P2, wave Dragon, and AquaBuoy.

WEC	Rated Power (kW)
Pelamis P2	750
Wave Dragon	7000
AquaBuoy	250

D. WAVE ENERGY CONVERTER LOCATION SUITABILITY (WLS) INDEX

The suitability of the location for the installation of the specific WEC can be identified using the wave energy convertor location suitability (WLS) index. The WLS index is computed from (14).

$$\text{WLS} = P_n + C_{fn} + d_n \tag{14}$$

P_n = Normalized mean wave power of the location, C_{fn} = Normalized capacity factor of the respective WEC, and dn = Normalized water depth of the location [41]. The parameters of the WLS index involve the normalized parameters and they are computed for each WEC separately as expressed by (15-17).

$$P_n = \frac{P_i}{P_{max}} \tag{15}$$

P_i = Mean wave power potential of location I, (kW/m) and P_{max} = Maximum mean wave power potential out of all study locations (kW/m) [41],

$$C_{fn} = \frac{C_{fi}}{C_{fmax}} \tag{16}$$

C_{fi} = Capacity factor at the location I, (%) and C_{fmax} = Maximum capacity factor of the respective WEC (%) [41],

$$d_n = 1 - (1 - d_{TH})\frac{d_i - d_{min}}{d_{max} - d_{min}} \tag{17}$$

d_{TH} = The threshold value assumed to be 0.3, d_i = Water depth of location I, (m), d_{min} = Minimum recommended depth for respective WEC (m) and d_{max} = Maximum water depth out of all study locations (m) [41].

Table 5 shows the minimum recommended depth for the three WECs studied here required for the parameter d_{min}. According to Sierra, *et al.*, if water depths of all study locations are greater than the minimum recommended depth of the WEC, then d_{min} would be the minimum water depths out of all the locations [41]. However, in this study, there are some locations with water depth lower than the minimum recommended depth of all WECs. Generally, they represent the locations where the only pipeline is working but not the jacket platform so they can be ignored for the energy calculations. Hence, the parameter d_{min} must be the minimum recommended depth for the respective WEC. Moreover, the study location with water depth less than the minimum recommended depth is considered where $d_n = 0$, as the water depth at the location is unable to meet the design requirement of the WEC.

TABLE 5. Minimum recommended depth for the WEC [42].

WEC	Min. recommended depth for WEC (m)
Pelamis P2	50
Wave Dragon	25
AquaBuoy	50

E. ENERGY OUTPUT FROM WAVE FARM

The power output of a WEC farm consisting of an array of WECs is expressed by (18). In a wave farm, energy losses in the processes of energy conversion should be considered. The parameter f_m considers the efficiency of the machinery

TABLE 6. (A)–(C) Significant wave height descriptive data statistics.

Peninsular Malaysia	H_S statistics (m)				$H_S > 2m$ (%)
	μ	Max	95%	σ	
1	1.31	6.0	2.5	0.63	9.22
2	1.31	6.0	2.5	0.63	9.22
3	1.29	5.0	2.5	0.61	8.50
4	1.37	5.0	2.5	0.64	9.24
5	1.40	5.0	3.0	0.66	11.31
6	1.40	5.0	3.0	0.66	11.31
7	1.41	5.0	3.0	0.66	11.36
8	1.09	4.5	2.0	0.50	2.95
9	1.21	4.5	2.5	0.57	6.16
10	1.31	5.5	2.5	0.63	9.22
11	1.31	5.5	2.5	0.63	9.22
12	1.31	5.5	2.5	0.63	9.22
13	1.31	5.5	2.5	0.63	9.22
14	1.44	5.0	3.0	0.66	11.92
15	1.44	5.0	3.0	0.66	11.92
16	1.32	5.0	2.5	0.63	9.20
17	1.14	4.5	2.0	0.53	4.48
18	1.22	4.5	2.5	0.56	6.06

(a)

Sarawak	H_S statistics (m)				$H_S > 2m$ (%)
	μ	Max.	95%	σ	
19	1.29	5.0	2.5	0.64	8.79
20	1.23	4.5	2.5	0.58	5.80
21	1.06	3.0	2.0	0.51	2.60
22	1.23	4.5	2.5	0.58	5.81
23	1.28	5.0	2.5	0.62	7.80
24	1.28	5.0	2.5	0.62	7.80
25	1.28	5.0	2.5	0.62	7.80
26	1.10	4.0	2.0	0.55	3.83
27	1.10	4.0	2.0	0.55	3.83
28	1.10	4.0	2.0	0.55	3.83
29	1.19	4.5	2.0	0.57	4.99
30	1.19	4.5	2.0	0.57	4.99
31	1.23	4.5	2.5	0.58	5.80
32	0.84	2.5	1.5	0.34	0.03
33	1.24	4.5	2.5	0.61	7.00
34	1.27	4.5	2.5	0.63	7.94
35	1.27	4.5	2.5	0.63	7.94
36	1.27	4.5	2.5	0.63	7.94
37	1.33	5.0	2.5	0.66	9.64
38	0.94	3.0	1.5	0.43	0.52
39	0.94	3.0	1.5	0.43	0.52

(b)

TABLE 6. *(Continued.)* (A) Significant wave height descriptive data statistics.

Sabah	H_S statistics (m)				H_S exceeding 2m (%)
	μ	Max.	95%	σ	
40	1.12	3.0	2.0	0.50	2.01
41	1.25	5.0	2.5	0.57	5.42
42	1.25	5.0	2.5	0.57	5.42
43	0.98	2.0	1.5	0.41	0.00
44	0.98	2.0	1.5	0.41	0.00
45	0.98	2.0	1.5	0.41	0.00
46	0.98	2.0	1.5	0.41	0.00
47	1.23	4.0	2.0	0.56	4.99
48	1.23	4.0	2.0	0.56	4.99
49	1.05	2.5	2.0	0.44	1.20
50	1.20	4.5	2.0	0.54	3.94
51	1.20	4.5	2.0	0.54	3.94

(c)

and is the ratio of the absorbed energy by the WEC to the mechanical energy of the power take-off (PTO) device. The f_e denotes the efficiency of mechanical energy being converted into electrical energy through the generator. Lastly, f_t denotes the efficiency of transmitting the electrical energy in a stable and useful form for power usage. The f_m and f_t are assumed to be 90 % while f_e is assumed to be 95 % [2],

$$P_f = nf_m f_e f_t P_E \tag{18}$$

P_f = Power output of wave farm (kW), n = Number of WECs, f_m = Efficiency of mechanical wave energy conversion, f_e = Efficiency of electrical energy conversion, and f_t = Efficiency of electrical energy transmission [2].

IV. DESCRIPTIVE STATISTICS OF SIGNIFICANT WAVE HEIGHT (H_S)

Descriptive statistics calculation on the significant wave height (H_S) was carried out for each individual location and the data from the scatter diagram was extracted as shown in Fig. 3. The main variables are the mean, maximum, 95th percentile, and standard deviation. Furthermore, the statistics for the percentage of H_S which exceeds the 2 m threshold are also computed.

Significant wave height (H_S) plays a very important role in the determination of energy from the ocean. Table 6 (A-C) shows the descriptive statistics of H_s the mean (μ), maximum, 95th percentile (95%), standard deviation (σ), and the percentage of H_S exceeding 2 m at each study location is taken as a threshold level. In the PMO region, the locations with the highest mean H_S of 1.44 m are 14-15. On the other hand, location 8 has the lowest mean H_S of 1.09 m. In the SKO region, 37 shows the highest mean H_S of 1.33 m while 32 shows the lowest mean H_S of 0.84 m. In the SBO region, locations 41 and 42 have the highest mean H_S of 1.25 m while locations 43-46 have the lowest mean H_S of 0.98 m.

TABLE 7. Mean wave power potential and annual mean wave power potential.

Peninsular Malaysia	Mean Wave Power Potential (kW/m)	Annual Mean Wave Power Potential (MWh/m)
1	6.81	59.62
2	6.81	59.62
3	5.78	50.62
4	6.65	58.23
5	7.09	62.10
6	7.09	62.10
7	7.16	62.70
8	3.62	31.67
9	3.50	30.65
10	6.81	59.62
11	6.81	59.62
12	6.81	59.62
13	6.81	59.62
14	7.44	65.13
15	7.44	65.13
16	6.05	52.95
17	5.18	45.40
18	4.94	43.32

(a)

Sarawak	Mean Wave Power Potential (kW/m)	Annual Mean Wave Power Potential (MWh/m)
19	7.63	66.86
20	6.61	57.91
21	4.78	41.88
22	5.80	50.80
23	7.44	65.18
24	7.44	65.18
25	7.44	65.18
26	5.40	47.28
27	5.40	47.28
28	5.40	47.28
29	6.09	53.33
30	6.09	53.33
31	5.80	50.80
32	2.45	21.44
33	7.07	61.94
34	7.34	64.30
35	7.34	64.30
36	7.34	64.30
37	8.10	70.95
38	3.41	29.87
39	3.41	29.87

(b)

TABLE 7. *(Continued.)* Mean wave power potential and annual mean wave power potential.

Sabah	Mean Wave Power Potential (kW/m)	Annual Mean Wave Power Potential (MWh/m)
40	5.33	46.70
41	6.62	57.98
42	6.62	57.98
43	3.47	30.36
44	3.47	30.36
45	3.47	30.36
46	3.47	30.36
47	6.44	56.45
48	6.44	56.45
49	3.30	28.88
50	5.99	52.47
51	5.99	52.47

(c)

Among the three regions, the highest mean H_S is found in the PMO region while the lowest is in the SKO region. When comparing the highest mean H_S between the regions, SKO gave a higher value than SBO, but SKO has a greater range of mean H_S as compared to both PMO and SBO.

Locations 14-15 have the highest percentage of H_S i.e., 11.92 % exceeding 2 m in the PMO region. Location 37, at 9.64 %, is the highest in the SKO region while locations 41-42, at 5.42 %, are the highest in the SBO region. Comparing the three regions, PMO shows a higher percentage of H_S exceeding 2 m.

A. MAXIMUM TO MEAN SIGNIFICANT WAVE HEIGHT RATIO

The ratio of maximum to mean H_S can be used to give an insight into the feasibility of wave energy. The maximum H_S could represent the investment cost incurred by the energy project while the mean H_S could represent the annual mean wave power available at that location [43]. Hence, the lower the ratio, the better the feasibility of the energy. Fig. 4 shows the lowest ratio in PMO is 3.5 at locations 7 and 15-16. Location 21 from SKO has the lowest ratio at 2.8 while locations 43-46 from SBO have a ratio of 2.0. Among the three regions, SBO with the lowest ratio may signify that wave energy development may be more economical as compared to the other regions.

B. MEAN SIGNIFICANT WAVE HEIGHT (H_S) AND MEAN WAVE PERIOD (T_e)

Fig. 5 (a-c) shows the mean H_S and mean T_e of the PMO, SKO, and SBO region, respectively. The trend of mean T_e

TABLE 8. Mean wave power potential generated by sea states.

Location	Mean Wave Power Potential (kW/m)	Percentage of H_S exceeding 2m (%)	Mean Wave Power by H_S exceeding 2 m (kW)	Percentage of Contribution (%)
1	6.81	9.22	2.21	32.5
2	6.81	9.22	2.21	32.5
3	5.78	8.50	1.76	30.5
4	6.65	9.24	2.12	31.9
5	7.09	11.31	2.5	35.3
6	7.09	11.31	2.5	35.3
7	7.16	11.36	2.54	35.5
8	3.62	2.95	0.55	15.2
9	3.50	6.16	1.23	35.2
10	6.81	9.22	2.21	32.5
11	6.81	9.22	2.21	32.5
12	6.81	9.22	2.21	32.5
13	6.81	9.22	2.21	32.5
14	7.44	11.92	2.71	36.4
15	7.44	11.92	2.71	36.4
16	6.05	9.20	1.94	32.1
17	5.18	4.48	0.98	18.9
18	4.94	6.06	1.21	24.5

(a)

Location	Mean Wave Power Potential (kW/m)	Percentage of H_S exceeding 2m (%)	Mean Wave Power by H_S exceeding 2 m (kW)	Percentage of Contribution (%)
19	7.63	8.79	2.2	28.8
20	6.61	5.80	1.36	20.6
21	4.78	2.60	0.53	11.1
22	5.80	5.81	1.24	21.4
23	7.44	7.80	1.95	26.2
24	7.44	7.80	1.95	26.2
25	7.44	7.80	1.95	26.2
26	5.40	3.83	0.95	17.6
27	5.40	3.83	0.95	17.6
28	5.40	3.83	0.95	17.6
29	6.09	4.99	1.15	18.9
30	6.09	4.99	1.15	18.9
31	5.80	5.80	1.24	21.4
32	2.45	0.03	0.01	0.4
33	7.07	7.00	2.67	37.8
34	7.34	7.94	1.97	26.8
35	7.34	7.94	1.97	26.8
36	7.34	7.94	1.97	26.8
37	8.10	9.64	2.49	30.7
38	3.41	0.52	0.10	2.9
39	3.41	0.52	0.10	2.9

(b)

in the PMO region is consistent, ranging from 4.0 s to 6.0 s. Only one location, namely location 9, has a mean T_e of lower than 4.0 s. Most of the mean T_e observed in SKO region range from 6.0 to 6.8 s, with only locations 22, 31, 32 with mean T_e lower than 6.0 s. In the SBO region, the mean T_e is found to be between 6.0 s to 7.0 s, with the only location 49 having a mean T_e of lower than 5.0 s.

TABLE 8. *(Continued.)* Mean wave power potential generated by sea states.

Location	Mean Wave Power Potential (kW/m)	Percentage of H_S exceeding 2m (%)	Mean Wave Power by H_S exceeding 2 m (kW)	Percentage of Contribution (%)
40	5.33	2.01	0.41	7.7
41	6.62	5.42	1.24	18.7
42	6.62	5.42	1.24	18.7
43	3.47	0.00	0.00	0.0
44	3.47	0.00	0.00	0.0
45	3.47	0.00	0.00	0.0
46	3.47	0.00	0.00	0.0
47	6.44	4.99	1.15	17.8
48	6.44	4.99	1.15	17.8
49	3.30	1.20	0.27	8.2
50	5.99	3.94	0.86	14.4
51	5.99	3.94	0.86	14.4

(c)

C. MEAN WAVE POWER POTENTIAL AND ANNUAL MEAN WAVE POWER POTENTIAL

Table 7 (A-C) shows the mean and annual mean wave power potential computed for the 51 study locations in the three regions. In the PMO region, locations 14-15 have the highest mean wave power potential at 7.44 kW/m. Location 37 from SKO has the highest mean wave power potential at 8.10 kW/m. Locations 41-42 have the highest mean wave power at 6.62 kW/m in the SBO region. Hence, SKO has the highest mean wave power potential amongst all the regions.

The locations with the highest mean wave power potential are also the locations with the highest mean H_S and the highest percentage of H_S exceeding 2 m recorded in Table 6. The high wave power potential detected in these locations can be related to the high H_S which significantly contributes to the wave power.

Taking 2 m as the threshold, the mean wave power contributed by waves with H_S exceeding 2 m is calculated. Table 8 (A-C) shows the mean wave power potential generated by sea states with H_S exceeding 2 m and its percentage of contribution to the total mean wave power. The overall mean wave power and the percentage of H_S exceeding 2 m of the location are also indicated. From Table 8, the highest mean wave power potential produced by sea states with H_S exceeding 2 m is 2.71 kW/m at locations 14-15. The lowest is at location 43-46 as the maximum H_S found at these locations

were only 2.0 m. In the individual regions, the highest values are 2.71 kW/m, 2.67 kW/m, and 1.24 kW/m for PMO, SKO, and SBO, respectively. The higher the percentage of H_S exceeding 2 m, the higher the mean power sea state will produce. However, that does not indicate that the higher percentage of H_S exceeding 2 m will mean a higher percentage of contribution to the overall mean wave power. This can be observed when the data of location 14-15 is compared with location 33. Although the former location had a higher percentage of H_S exceeding 2 m, thus a higher mean power produced by the sea state, the mean power produced contributed less to the overall mean power potential as compared to the latter.

D. DIRECTIONAL WAVE DATA

The wave rose diagram of the locations with the highest mean wave power location 14-15, 37, 41-42, were studied for further analysis of the energy production. Fig. 6(a) shows the wave rose in terms of percentage of occurrence for location 14- 15 while Fig. 6(b) and 7(c) show for location 37 and locations 41-42, respectively.

From Fig. 6(a-c), it can be observed that the direction of the high percentage of significant wave height is from the North and the Northeast direction for all the locations. This relates to the seasonal Northeast monsoon, from November to the end of February. It can also be noted that the H_S at locations 15-16 (PMO region) comes from the South while locations 37 and 41-42 (SKO and SBO region, respectively) comes from the West.

V. WAVE ENERGY CONVERTER (WEC) PERFORMANCE

The performance of the WECs, i.e., the Pelamis P2, Wave Dragon, and AquaBuoy, is determined when they are deployed at the study locations.

A. ESTIMATED ELECTRICAL OUTPUT

Table 9 (A-C) shows the estimated mean output produced from the three WECs, assuming the WECs function for 8760 hours in a year. From Table 9, the Pelamis P2 produces the highest output at locations 14-15, 37, 41-42 at PMO, SKO, and SBO region, respectively. The electricity output is 87.98 kW/m, 106.86 kW/m, and 92.57 kW/m, respectively. For the Wave Dragon, the highest output is found at locations 1-2, 10-13 at the PMO region. The highest output found in the regions of SKO and SBO is at locations 37 and 41-42, respectively. The electricity outputs are 5159.73 kW/m, 6478.55 kW/m, and 5636.71 kW/m for PMO, SKO, and SBO regions, respectively. The highest output found for the AquaBuoy is the same location as the Wave Dragon. The electricity output is 15.66 kW/m, 21.00 kW/m, 16.90 kW/m, respectively.

B. CAPACITY FACTOR

The Capacity Factor parameter C_f is used to assess and compare the efficiency of different WECs with different rated power. The higher the C_f the better the WEC is utilized to its

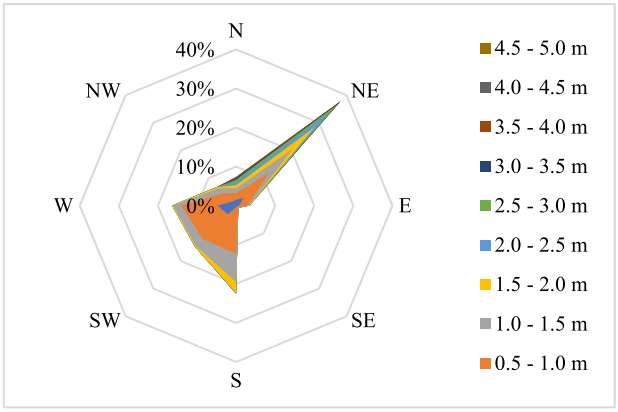

(a) Wave rose for location 14 and 15..

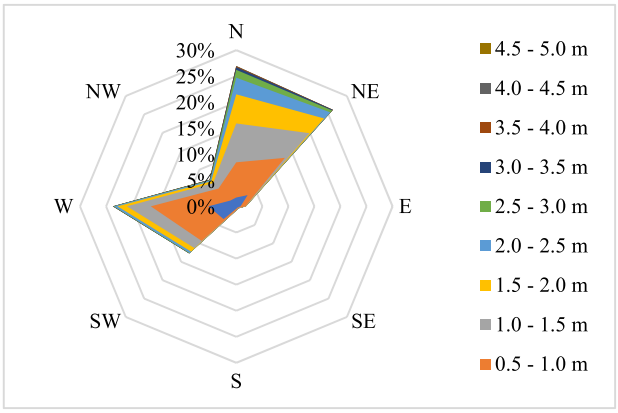

(b) Wave rose for location 37.

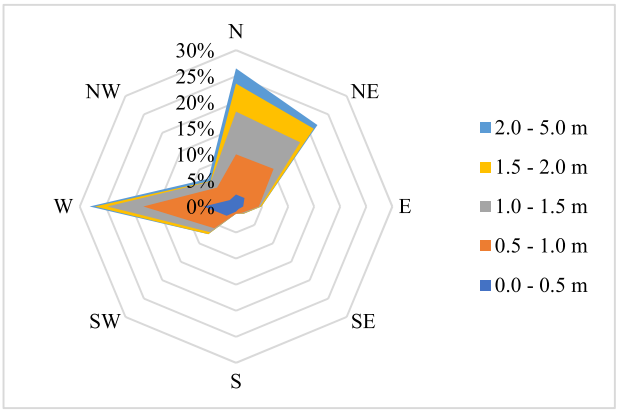

(c) Wave rose for location 41 and 42.

FIGURE 6. (a). Wave rose for location 14 and 15. (b). Wave rose for location 37. (c). Wave rose for location 41 and 42.

abilities. Fig. 11 shows the C_f of the three WECs, Pelamis P2, Wave Dragon, and AquaBuoy, when they are deployed at the study locations. From Fig 11, the highest C_f of 14.2 % is achieved by Pelamis P2 at location 37. In the individual regions, the highest C_f of 11.7 % (location 14-15), 14.2% (location 37), and 12.3% (location 41-42) are achieved in the PMO, SKO, and SBO regions, respectively, all by the Pelamis P2. The aforementioned locations are also those with the highest mean wave power recorded in Table 8.

Overall, the Pelamis P2 achieved a higher C_f throughout all the study locations as compared to the Wave Dragon and the

TABLE 9. (A)–(C) Estimated mean output and mean annual output.

PMO	Mean output (kW)	Mean annual output (MWh)	Mean output (kW)	Mean annual output (MWh)	Mean output (kW)	Mean annual output (MWh)
	Pelamis P2		Wave Dragon		AquaBuoy	
1	87	764	589	5160	16	137
2	87	764	589	5160	16	137
3	68	597	463	4052	11	95
4	78	686	516	4522	13	117
5	85	745	549	4805	15	128
6	85	745	549	4805	15	128
7	85	743	555	4861	15	129
8	35	302	289	2535	5	42
9	15	129	76	664	0.1	1
10	87	764	589	5160	16	137
11	87	764	589	5160	16	137
12	87	764	589	5160	16	137
13	87	764	589	5160	16	137
14	88	771	573	5018	15	135
15	88	771	573	5018	15	135
16	70	618	481	4210	11	99
17	72	634	514	4501	13	109
18	56	489	401	3516	8	74

(a)

SKO	Mean output (kW)	Mean annual output (MWh)	Mean output (kW)	Mean annual output (MWh)	Mean output (kW)	Mean annual output (MWh)
	Pelamis P2		Wave Dragon		AquaBuoy	
19	102	890	710	6215	20	173
20	91	800	645	5647	17	149
21	91	800	645	5647	17	149
22	91	800	645	5647	17	149
23	66	579	514	4504	12	103
24	66	579	514	4504	12	103
25	66	579	514	4504	12	103
26	70	617	542	4749	13	110
27	100	872	698	6118	19	168
28	70	616	540	4733	13	113
29	85	741	606	5310	16	137
30	85	741	606	5310	16	137
31	70	617	542	4749	13	110
32	30	266	339	2968	4	37
33	83	730	634	5554	15	134
34	98	861	690	6045	19	166
35	98	861	690	6045	19	166
36	98	861	690	6045	19	166
37	107	936	740	6479	21	184
38	48	420	423	3709	8	68
39	48	420	423	3709	8	68

(b)

SBO	Mean output (kW)	Mean annual output (MWh)	Mean output (kW)	Mean annual output (MWh)	Mean output (kW)	Mean annual output (MWh)
	Pelamis P2		Wave Dragon		AquaBuoy	
40	72	633	553	4846	13	113
41	93	811	643	5637	17	148
42	93	811	643	5637	17	148
43	51	442	416	3644	8	70
44	51	442	416	3644	8	70
45	51	442	416	3644	8	70
46	51	442	416	3644	8	70
47	90	788	636	5575	17	145
48	90	788	636	5575	17	145
49	28	242	246	2154	3	23
50	85	747	605	5301	15	135
51	85	747	605	5301	15	135

(c)

AquaBuoy. There is only one occasion, at location 32, where the Wave Dragon achieved a higher C_f than the Pelamis P2. From the scatter diagram of location 32, it is noted that the most frequently occurring sea states are when $H_S \leq 0.5$ m. A similar occurrence can be found in other locations such as locations 26-28, 38-39, 43-46. However, location 32 had a much higher density of occurrence at the said sea state. This causes the estimated output from Pelamis P2 to be lower as according to its power matrix, the WEC produces zero output at $H_S \leq 0.5$ m. This could be the reason why Pelamis P2 had a lower C_f than the Wave Dragon at location 32.

VI. BEST SUITED LOCATION

In this section, the best suited location out of the 51 locations for wave energy development is evaluated based on the WLS index.

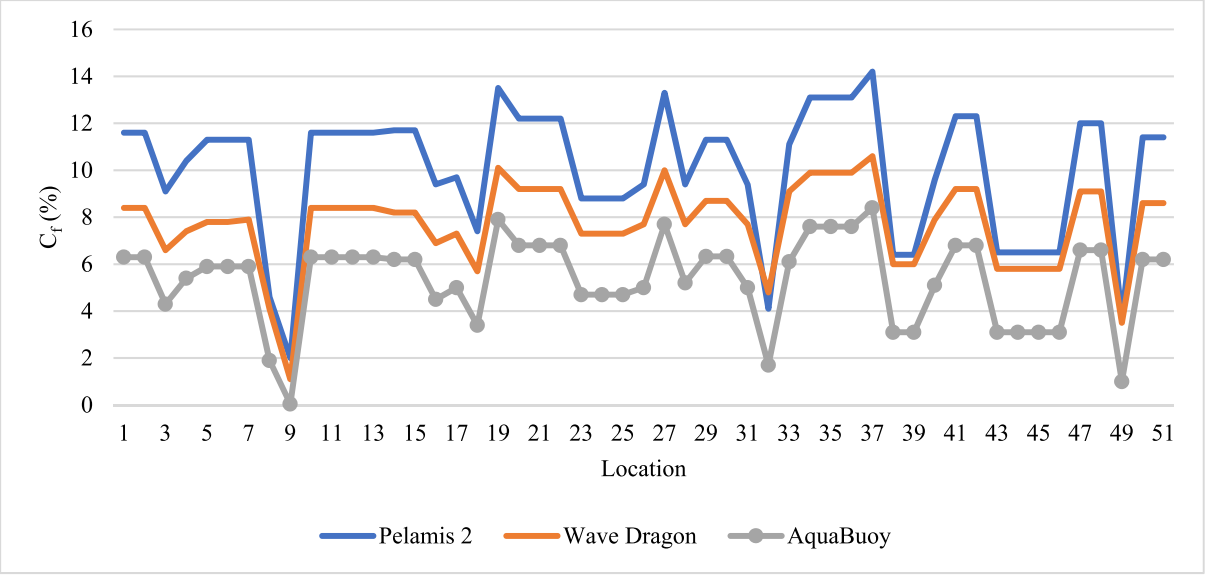

FIGURE 7. Capacity factor of WECs computed for all study locations.

A. NORMALIZED PARAMETERS

Table 10 (A-C) shows the normalized parameters, P_n, C_{fn}, and d_n, involved in the decision of choosing the best suited location for wave energy development. Since both C_{fn} and d_n are WEC dependent parameters, they are calculated according to the respective WECs. The greater the value of the normalized parameters, the better the feasibility of the location. The data in the third column within each WEC column shows the sum of c_{fn} and d_n of the respective WECs. From Table 10, the highest P_n can be found in locations 14-15, 37, and 41-42, for PMO, SKO, and SBO regions, respectively. The value of P_n for these locations are 0.92, 1.00, and 0.82, respectively. Hence, location 37 holds the highest P_n for all regions. This is in parallel with the results of mean wave power, where location 37 gave the highest mean wave power potential amongst all other locations.

The normalized parameters, C_{fn}, and d_n are WEC-dependent variables. Hence, the sum of the same WEC should be taken to identify the best WEC option for a particular location. Since the greater, the value of normalized parameters, the better the feasibility, the WEC that gives the larger sum of C_f and d_n is taken as the better option for that particular location. Fig. 12 shows the sum of C_{fn} and d_n of the three WECs when they are deployed at different locations.

In general, the sum of C_{fn} and d_n for the Pelamis P2 is the highest among the three WEC at the majority of the locations. There are occasions when the sum for Wave Dragon is the highest. There are 14 of the said occasions, found at locations 26-30, 32, 34-35, 38-39, and 45-48. Upon closer inspection, it is observed most of these locations have water depths that do not meet the minimum required depth for the Pelamis P2. Thus, these locations will have a d_n value of 0.0 and a lower overall sum of C_{fn} and d_n for the Pelamis P2 than that for the Wave Dragon. Location 34-36 met the requirement but is close to the borderline, hence having a low d_n value.

Thus, the Wave Dragon is said to be more suitable to be deployed at locations 26-30, 32, 34-35, 38-39, and 45-48 while the Pelamis P2 is more suitable to be deployed at the remaining locations. From Fig. 12, the Pelamis P2 is observed to be most suited for location 20, achieving the summation value of 1.85. The Wave Dragon is found to be most suited for location 27 with a summation value of 1.91 while the AquaBuoy is found to be most suited for location 20 with a summation value of 1.80.

B. WAVE ENERGY CONVERTER LOCATION SUITABILITY

To choose the best suited location from all the study locations, the best option for each location is taken into consideration. The sum of the three variables, P_n, C_{fn}, and d_n is presented in Fig. 8. The greater the value of WLS index, the better the suitability of the location for wave energy development.

From Fig. 7, the location with the highest WLS index in the PMO region is location 2, with WLS index of 2.50. Location 20 from SKO and location 48 from SBO have the highest WLS index for their respective regions, with WLS index of 2.67 and 2.54, respectively. All of these locations are shown in Fig. 9 which shows the exact location of the area where the wave energy converter can be installed. Fig. 9 also shows all locations of the platforms in Malaysia. Legends indicating yellow are related to the Peninsular Malaysia, green indicates platforms from Sabah and Purple indicates platforms from Sarawak. Fig. 10 shows the WLS index for all locations. In overall, location 20 from SKO has the highest WLS index. From this result, location 20 is said to be the best suited location for offshore wave energy development. As determined earlier the Pelamis P2 is evaluated to be the

TABLE 10. (A) Normalized parameters for different WECS. (B) Normalized parameters for different WECS. (C) Normalized parameters for different WECS.

PMO	P_n	Pelamis P2			Wave Dragon			AquaBuoy		
		C_{fn}	d_n	Sum	C_{fn}	d_n	Sum	C_{fn}	d_n	Sum
1	0.84	0.82	0.8	1.65	0.79	0.6	1.44	0.75	0.8	1.58
2	0.84	0.82	0.8	1.66	0.79	0.6	1.44	0.75	0.8	1.59
3	0.71	0.64	0.6	1.26	0.62	0.5	1.13	0.51	0.6	1.13
4	0.82	0.73	0.6	1.34	0.70	0.5	1.20	0.64	0.6	1.25
5	0.88	0.80	0.6	1.39	0.74	0.5	1.22	0.70	0.6	1.29
6	0.88	0.80	0.6	1.41	0.74	0.5	1.24	0.70	0.6	1.32
7	0.88	0.80	0.7	1.46	0.75	0.5	1.28	0.70	0.7	1.37
8	0.45	0.32	0.8	1.17	0.39	0.7	1.04	0.23	0.8	1.07
9	0.43	0.14	0.5	0.69	0.10	0.5	0.56	0.00	0.5	0.55
10	0.84	0.82	0.6	1.40	0.79	0.5	1.28	0.75	0.6	1.34
11	0.84	0.82	0.7	1.51	0.79	0.6	1.34	0.75	0.7	1.44
12	0.84	0.82	0.8	1.60	0.79	0.6	1.40	0.75	0.8	1.54
13	0.84	0.82	0.7	1.47	0.79	0.5	1.32	0.75	0.7	1.40
14	0.92	0.82	0.6	1.42	0.77	0.5	1.27	0.74	0.6	1.34
15	0.92	0.82	0.6	1.40	0.77	0.5	1.25	0.74	0.6	1.32
16	0.75	0.66	0.8	1.43	0.65	0.6	1.25	0.54	0.8	1.30
17	0.64	0.68	0.7	1.43	0.69	0.6	1.27	0.60	0.7	1.34
18	0.61	0.52	0.8	1.37	0.54	0.7	1.19	0.40	0.8	1.25

(a)

SKO	P_n	Pelamis P2			Wave Dragon			AquaBuoy		
		C_{fn}	d_n	Sum	C_{fn}	d_n	Sum	C_{fn}	d_n	Sum
19	0.94	0.95	0.7	1.62	0.95	0.5	1.49	0.94	0.7	1.61
20	0.82	0.86	1.0	1.85	0.87	0.7	1.61	0.81	1.0	1.80
21	0.59	0.86	0.0	0.86	0.87	0.0	0.87	0.81	0.0	0.81
22	0.72	0.86	1.0	1.83	0.87	0.7	1.60	0.81	1.0	1.78
23	0.92	0.62	0.6	1.24	0.69	0.5	1.19	0.56	0.6	1.18
24	0.92	0.62	0.7	1.28	0.69	0.5	1.22	0.56	0.7	1.22
25	0.92	0.62	0.7	1.35	0.69	0.6	1.27	0.56	0.7	1.29
26	0.67	0.66	0.0	0.66	0.73	0.9	1.63	0.60	0.0	0.60
27	0.67	0.94	0.0	0.94	0.94	1.0	1.91	0.92	0.0	0.92
28	0.67	0.66	0.0	0.66	0.73	0.8	1.53	0.62	0.0	0.62
29	0.75	0.80	0.0	0.80	0.82	0.8	1.61	0.75	0.0	0.75
30	0.75	0.80	0.0	0.80	0.82	0.8	1.62	0.75	0.0	0.75
31	0.72	0.66	0.9	1.54	0.73	0.7	1.40	0.60	0.9	1.47
32	0.30	0.29	0.0	0.29	0.45	0.0	0.45	0.20	0.0	0.20
33	0.87	0.78	1.0	1.75	0.86	0.7	1.59	0.73	1.0	1.70
34	0.91	0.92	0.3	1.22	0.93	0.3	1.23	0.90	0.3	1.20
35	0.91	0.92	0.3	1.22	0.93	0.3	1.23	0.90	0.3	1.20
36	0.91	0.92	0.3	1.23	0.93	0.3	1.24	0.90	0.3	1.21
37	1.00	1.00	0.3	1.32	1.00	0.3	1.31	1.00	0.3	1.32
38	0.42	0.45	0.0	0.45	0.57	1.0	1.55	0.37	0.0	0.37
39	0.42	0.45	0.0	0.45	0.57	1.0	1.57	0.37	0.0	0.37

(b)

TABLE 10. *(Continued.)* (A)–(C) Normalized parameters for different WECS.

SBO	P_n	Pelamis P2			Wave Dragon			AquaBuoy		
		C_{fn}	d_n	Sum	C_{fn}	d_n	Sum	C_{fn}	d_n	Sum
40	0.66	0.68	0.9	1.57	0.75	0.7	1.43	0.61	0.9	1.50
41	0.82	0.87	0.8	1.71	0.87	0.7	1.52	0.81	0.8	1.65
42	0.82	0.87	0.8	1.71	0.87	0.7	1.52	0.81	0.8	1.65
43	0.43	0.46	0.0	0.46	0.55	0.8	1.33	0.37	0.0	0.37
44	0.43	0.46	1.0	1.42	0.55	0.7	1.27	0.37	1.0	1.33
45	0.43	0.46	0.0	0.46	0.55	0.0	0.55	0.37	0.0	0.37
46	0.43	0.46	0.0	0.46	0.55	0.0	0.55	0.37	0.0	0.37
47	0.80	0.85	0.0	0.85	0.86	0.8	1.68	0.79	0.0	0.79
48	0.80	0.85	0.0	0.85	0.86	0.9	1.74	0.79	0.0	0.79
49	0.41	0.26	0.9	1.15	0.33	0.7	1.01	0.12	0.9	1.00
50	0.74	0.80	0.9	1.66	0.81	0.7	1.47	0.74	0.9	1.60
51	0.74	0.80	1.0	1.75	0.81	0.7	1.53	0.74	1.0	1.69

(c)

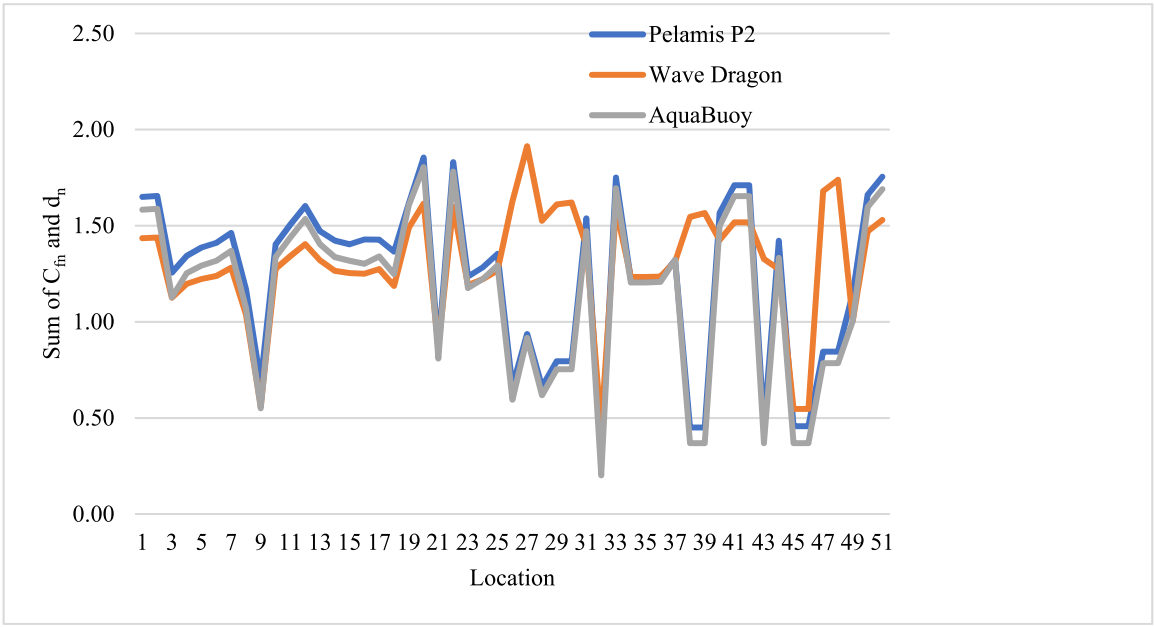

FIGURE 8. Sum of C_{fn} and d_n for the three WECs when deployed at different study locations.

best WEC option to be deployed to harvest the wave energy at location 20.

VII. WEC FEASIBILITY ANALYSIS

It has already been found that location 20 is identified to be the best suited location for wave energy development and the Pelamis P2 is determined to be the best WEC option for that location. Now the feasibility of the wave energy project assuming it takes place at location 20, using the Pelamis P2 is assessed based on its energy supply, environmental benefits, and economic impacts.

A. ENERGY SUPPLY

The energy demand typically ranges from 10-50 MW. Hence, 10 MW is taken as the minimum while 50 MW is taken as the maximum value for the offshore platforms. From Table 9, when one unit of Pelamis P2 is deployed at location 20, the energy output is estimated to be 91.37 kW or 800.40 MWh/ yr. From these results, one unit of the Pelamis

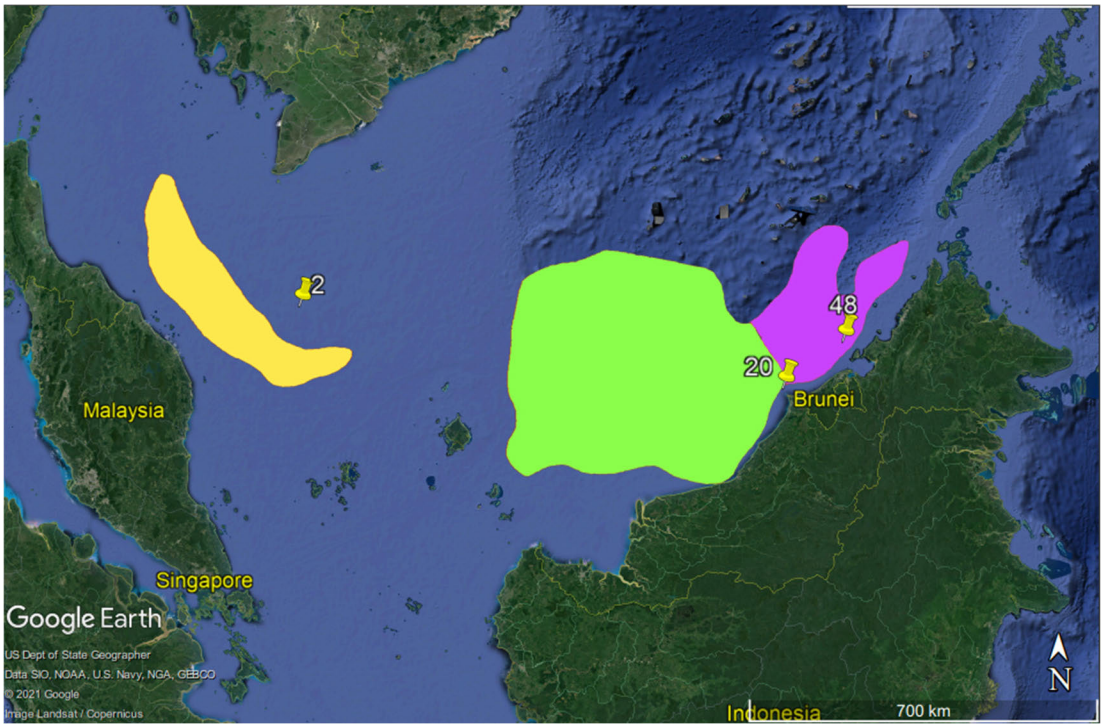

FIGURE 9. Google Earth map showing the best suited locations for offshore wave energy development in the SCS. The shaded regions are obtained from an online source to indicate the area of the regions [42].

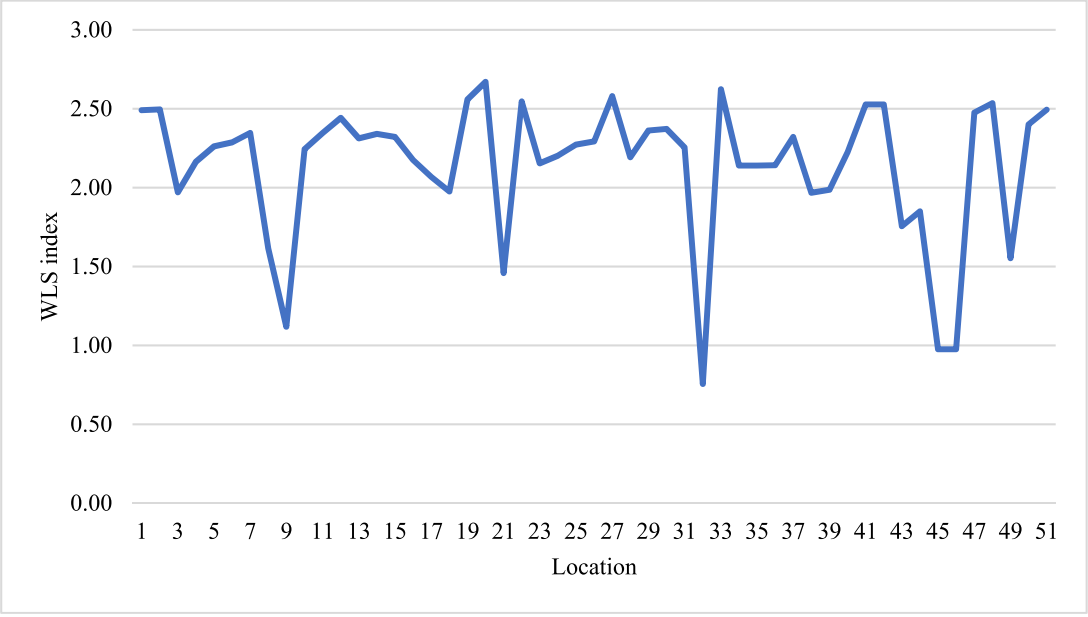

FIGURE 10. WLS index computed for all study locations.

P2 will only be able to supply 0.18-0.91 % of the platform's demand, which is very low and insufficient. To overcome this issue, the project needs to utilize multiple units of WECs as an array or a wave farm to increase the energy output. Hence, an assessment of the energy supply for a single unit, 10 units, 50 units, and 100 units is conducted.

B. ENVIRONMENTAL BENEFITS OF THE PROJECT

The environmental benefits of the project are evaluated based on the amount of fossil fuels that can be replaced when wave energy is utilized as a part of the energy supply. Based on a survey conducted by Statista Research Department in the US, it is said that 1000 ft^3 of natural gas can produce 99 kWh of

TABLE 11. Summary of assessment outcome for different units of Pelamis P2 WEC installed at location 20.

Unit	Output/unit (kW)	Output (kW)	Annual Ouput/ unit (MWh/ yr)	Annual Output (MWh/ yr)	Percentage of energy supply (%) For min. demand (10 MW)	For max. demand (50 MW)	Natural gas reduction (m^3/ yr)	Savings from natural gas reduced (mil RM/ yr)	CO reduction (tonnes/ yr)	NOx reduction (tonnes/ yr)
1	91.37	91.37	800.4	800.4	0.91	0.18	228937	264	161	698
10	91.37	703.1	800.4	6159	7.0	1.4	1761672	2033	1240	5373
50	91.37	3515.5	800.4	30795	35.2	7.0	8808359	10167	6199	26863
100	91.37	7030.9	800.4	61591	70.3	14.1	17616717	20334	12398	53727

electricity [44]. In other words, approximately 0.286 m^3 of natural gas produces 1 kWh of electricity. According to this, the amount of natural gas that can be reduced annually can be calculated. One unit of Pelamis P2 produces 800.40 MWh of electricity every year. Thus, approximately 230000 m^3 of natural gas can be avoided every year.

From the United States Environmental Protection Agency (USEPA), assuming that the platforms are equipped with water-steam injection emission control, the emission factors of CO and NOx from the natural gas fired turbine are 0.13 lb/mm BTU and 0.03 lb/mm BTU, respectively [46]. Assuming that the energy content of natural gas is 55 MJ/kg [47], 230000 m^3 of natural gas reduction can avoid the emission of approximately 160 tonnes of CO and 700 tonnes of NOx annually.

C. ECONOMIC BENEFITS OF THE PROJECT

According to the Edge Market website, the average selling price of natural gas for Q1 of 2021 is RM 22.14/ mm Btu or RM 1.15/ kJ when the energy content of natural gas is 55 MJ/ kg [48]. With every 230000 m^3 of natural gas avoided every year, the project can achieve fuel savings up to RM 260 million in a year.

Table 11 shows the summary of the assessment conducted for a single unit, 10 units, 50 units, and 100 units of the Pelamis P2 WEC. From Table 11, it can be observed that with 100 units of Pelamis P2 installed, the project can supply almost 70.3 % of the energy supply if the minimum requirement is considered while 14.1 % of the energy supply can be achieved when the maximum requirement is considered. Consequently, the project would save up to 17.6E06 m^3 natural gas, avoiding almost 12000 tonnes of CO and 54000 tonnes of NOx.

VIII. COMPARISON WITH OTHER PUBLISHED STUDIES

Table 12 shows a comparison between previous studies from the South China Sea. One important difference is that most of these studies are conducted near the coastal region, island, or main sea, and no study was found near the oil and gas platforms, which are found near Malaysia, Thailand, Indonesia, and Vietnam. It can be found from the Table that the wave energy determined in this region is comparable to all other studies conducted in this region. Baristow has reported that most energy-rich areas of the global oceans are in the mid to high latitude temperate storm belts of both hemispheres, between 40 and 60° [49]. In equatorial waters, we find power levels of 15-20 kW/m on an annual basis over parts of all the ocean basins. There are also large seasonal changes in the monsoon areas of South East Asia due to the seasonal switch in wind direction in these areas. This is particularly large along seasonally downwind and upwind coastlines due to the influence of fetch on wind wave growth and is particularly strong in the South China Sea since there is little swell to smooth out these seasonal wind sea changes. Finally, the relationship between the extreme and mean significant wave heights is important i.e., the lower this ratio is, the more feasible a wave energy project might be as the extreme conditions related to design and to a certain extent operational costs and the mean represents the resource or the income [49].

When wave power flux exceeds 2 kW/m, it is usually considered as an available energy resource to be harvested. The seas where the value is over 10 kW/m is recognized as energy-rich regions of wave energy resource [50]. The effective wave height was defined by [54] for the first time, which significantly improve our knowledge on the availability of wave energy. In the wave energy development, the wave height higher than 1.3 m is considered as the available wave height. The wave height higher than 4 m has great destructive power and is not conducive to the operation and safety of the wave power equipment. The wave height available for wave development is limited between 1.3-4 m, known as the effective wave height.

The wave energy of the research region is mainly contributed by the following sea states: wave height 2–3 m and wave period 6–7 s, contribution rate 14.6%; wave height 2–3 m and wave period 7–8 s, contribution rate 11.1%;

TABLE 12. Annual Mean Wave power in different parts of South China Sea.

Site names	Location (Longitude-Latitude)	Depth (m)	Annual (kW/m)
This study	3.8-6.3 N – 103.3-115.7 E	6-95	6.61
Hameau Mo, Vietnam	109.53 E - 12.90 N	160	10.57 [52]
Spratly Island	114.37 E - 11.53 N	1870	14.74 [52]
Cape Bolinao, Philippines	119.46 E - 16.36 N	1680	6.70 [52]
Palawan, Philippines	117.23 E - 08.70 N	42	6.30 [52]
Brunei	115.16 E - 05.50 N	20	3.15 [52]
Sarawak, Malaysia	109.70 E - 02.13 N	23	2.86 [52]
Redang, Malaysia	103.07 E - 05.80 N	14	2.48 [52]
Ko Samui, Thailand	100.10 E - 09.47 N	10	0.67 [52]
Duyen Hai, Vietnam	106.70 E - 09.57 N	18	2.00 [52]
Korean Peninsula	117-143E 20-50N	41-150	6-10 [39]
Equatorial waters	Equator	-	15-20 [49]
East China Sea and South China Sea	0°–41°N, 97°E–135°E	-	Over 2.0 [53]
South China Sea			4–20 [54]
South China Sea	118.83-128.63 E 21.04-33.08 N		9.6-20 [55]
South China Sea	115°35'- 116°26' To 22°16'- 22°52'	-	10 to 18 kW/m [48]
Japan Coast	130-145 E- 32-40N	29	4-10 [56]

wave height 1–2 m and wave period 5–6 s, contribution rate 9.1%; wave height 3–4 m and wave period 8–9 s, contribution rate 8.1% [51]. The SCS is a partially-enclosed sea basin covering an area in the north of the Taiwan Strait, and in the south to Karimata Strait. China, Vietnam, the Philippines, Malaysia, Brunei, Thailand, Indonesia, and Cambodia share its boundary. The weather of the SCS is strongly influenced by the two monsoon seasons, summer (southwest) and winter (northeast). Zheng *et al.* [53] evaluated the wind and wave power resources in the East and the South China Sea. The research categorised the regions into four groups of wave power, i.e., ''indigent area'' (<1 kW/m), ''available area'' (<1-6 kW/m), ''subrich area'' (6-15 kW/m), and ''rich area'' (>15 kW/m). The southern part of the SCS, like the Gulf of Thailand, Karimata, and Malacca Straits were grouped as ''indigent areas''. Other southern regions of the SCS are classified as ''available areas'', and the central region of SCS was grouped as ''subrich area''. There is no region to be classified in SCS as a ''rich area'' Zheng et al [54]. It can be seen that the annual wave energy of 6.61 kW/m near the jacket platforms in offshore Malaysia is very competitive as compared to the other studies.

IX. CONCLUSION

In this study, the assessment of wave energy in the SCS offshore of Malaysia was conducted. Among 51 study locations, locations 14-15, 37, and 41-42 were identified to have the highest mean wave power potential at PMO, SKO, and SBO regions, respectively. The locations gave the potential of 7.44 kW/m, 8.10 kW/m, and 6.62 kW/m. These locations are also the same locations that showed the highest mean H_S among the other locations of their respective regions. This result suggests that more wave energy can be generated from these locations as compared to the other locations. However, wave energy is harvested with the use of devices known as WECs, which may work at different efficiency depending on their design. Hence, the selection of best suited location needs to be considered for the WEC performance.

Based on the WLS index, locations 2, 20, and 48 were identified as the best suited location for offshore wave energy development in the PMO, SKO, and SBO regions, respectively. Location 20 was determined to be the best location for wave energy development with the highest WLS index of 2.67. In addition to that, the Pelamis P2 was found to be the most suited WEC to be installed in location 20. The characteristics of location 20 are that it is 50.3 m deep, and has a potential mean wave power of 6.61 kW/m. One unit of Pelamis P2 can produce approximately 91.37 kW/m of electricity and achieve up to 12.2 % of Cf when it is deployed at location 20.

Based on the electricity output of Pelamis P2 at location 20, the energy supply can only supply 0.91 % of the platform's minimum energy demand and 0.18 % of the maximum demand. A wave farm consisting of 100 units of Pelamis P2 could generate electricity up to 62 GWh/yr, which will be able to meet 70.3 % of the minimum energy demand or 14.1 % of the maximum energy demand. Furthermore, the wave farm could also reduce the use of natural gas up to 17.6E06 m^3/ yr. This leads to the reduction of approximately 12000 tonnes of CO and 54000 tonnes of NOx annually. At the same time, the wave farm can save up to RM 20 billion in a year.

REFERENCES

[1] L. Kramer. (2020). *Upstream Vs. Downstream Oil & Gas Operations: What's the Difference?*. [Online]. Available: https://www.investopedia.com/aSKO/answers/060215/what-difference-between-upstream-and-downstream-oil-and-gas-operations.asp

[2] S. Oliveira-Pinto, P. Rosa-Santos, and F. Taveira-Pinto, ''Electricity supply to offshore oil and gas platforms from renewable ocean wave energy: Overview and case study analysis,'' *Energy Convers. Manage.*, vol. 186, pp. 556–569, Apr. 2019.

[3] B. Jiang, G. Wu, J. Ding, C. Ma, Y. Fang, and X. Wang, ''Assessment of the wave energy resource in the South China sea,'' *Proc. Inst. Civil Eng.-Maritime Eng.*, vol. 172, no. 1, pp. 23–33, Mar. 2019.

[4] C. W. Zheng, Q. Su, and T. J. Liu, "Wave energy resources assessment and dominant area evaluation in the China sea from 1988 to 2010," *Acta Oceanol. Sinica*, vol. 35, no. 3, pp. 104–111, 2013, doi: 10.1680/jmaen.2018.29.
[5] United Nations. (2020). *United Nation Sustainable Development Goals*. [Online]. Available: https://www.un.org/sustainabledevelopment/energy/
[6] W. S. W. Abdullah, M. Osman, M. Z. A. Ab Kadir, and R. Verayiah, "The potential and status of renewable energy development in Malaysia," *Energies*, vol. 12, no. 12, p. 2437, Jun. 2019.
[7] N. S. Eusoff. (2018). *Malaysia Sets New Goal of 20% Clean Energy Generation by 2030*. [Online]. Available: https://www.theedgemarkets.com
[8] M. Ragazzi, G. Ionescu, and S. I. Cioranu, "Assessment of environmental impact from renewable and non-renewable energy sources," *Int. J. Energy Prod. Manage.*, vol. 2, no. 1, pp. 8–16, 2017.
[9] T.-V. Nguyen, M. Voldsund, P. Breuhaus, and B. Elmegaard, "Energy efficiency measures for offshore oil and gas platforms," *Energy*, vol. 117, pp. 325–340, Dec. 2016.
[10] IEA. (2019). *Renewables*. [Online]. Available: https://www.iea.org/reports/renewables-2019
[11] K. Narula, *The Maritime Dimension of Sustainable Energy Security*. Singapore: Springer, 2019.
[12] M. Fadli. (2019). *Oil and Gas Reserves Can Last 10 Years*. [Online]. Available: https://www.freemalaysiatoday.com/category/nation/2019/03/13/oil-and-gas-reserves-can-last-10-years-dewan-rakyat-told/
[13] S. Tata. (2017). *Deconstructing China's Energy Security Strategy*. [Online]. Available: https://thediplomat.com/2017/01/deconstructing-chinas-energy-security-strategy/.
[14] The Economic Times. (2019). *India's Oil Import Dependece Jumps to 84 Per Cent*. [Online]. Available: https://economictimes.indiatimes.com/industry/energy/oil-gas/indias-oil-import-dependence-jumps-to-84-pc/articleshow/69183923.cms?from=mdr
[15] Eurostat. (2020). *Energy Production and Imports*. [Online]. Available: https://ec.europa.eu/eurostat/statisticsexplained/
[16] M. Siddi, "The EU's energy union: A sustainable path to energy security?" *Int. Spectator*, vol. 51, no. 1, pp. 131–144, Apr. 2016.
[17] U. Shahzad, "The need for renewable energy sources," *Int. J. Inf. Technol. Electr. Eng.*, vol. 4, no. 4, pp. 16–18, 2015.
[18] H. Liming, "Financing rural renewable energy: A comparison between China and India," *Renew. Sustain. Energy Rev.*, vol. 13, no. 5, pp. 1096–1103, Jun. 2009.
[19] Y. K. Tiong, M. A. Zahari, S. F. Wong, and S. S. Dol, "The feasibility of wind and solar energy application for oil and gas offshore platform," in *Proc. 9th Curtin Univ. Technol. Sci. Eng. Int. Conf.*, Malaysia, 2015.
[20] A. R. Årdal, K. Sharifabadi, Ø. Bergvoll, and V. Berge, "Challenges with integration and operation of offshore oil & gas platforms connected to an offshore wind power plant," in *Proc. Petroleum Chem. Ind. Conf. Eur.*, Amsterdam, The Netherlands, Jun. 2014, pp. 1–9.
[21] A. Zhang, H. Zhang, M. Qadrdan, W. Yang, X. Jin, and J. Wu, "Optimal planning of integrated energy systems for offshore oil extraction and processing platforms," *Energies*, vol. 12, no. 4, p. 756, Feb. 2019.
[22] M. Korpås, L. Warland, W. He, and J. O. G. Tande, "A case-study on offshore wind power supply to oil and gas rigs," *Energy Procedia*, vol. 24, pp. 18–26, 2012.
[23] A. Pecher and J. P. Kofoed, *Handbook of Ocean Wave Energy*. Cham, Switzerland: Springer, 2017.
[24] R. Waters, "Energy from ocean waves: Full scale experimental verification of a wave energy converter," Summaries Uppsala Dissertations Fac. Sci. Technol., Uppsala Univ., Uppsala, Sweden, Tech. Rep. 580, 2008.
[25] F. Mwasilu and J. W. Jung, "Potential for power generation from ocean wave renewable energy source: A comprehensive review on state-of-the-art technology and future prospects," *IET Renew. Power Gener.*, vol. 13, no. 3, pp. 363–375, 2019.
[26] T. Aderinto and H. Li, "Review on power performance and efficiency of wave energy converters," *Energies*, vol. 12, no. 22, p. 4329, Nov. 2019.
[27] L. Christensen, E. Friis-Madsen, and J. P. Kofoed, "The wave energy challenge: The wave dragon case," in *Proc. POWER-GEN Eur. Conf.*, Milan, Italy, Jun. 2005, pp. 1–21.
[28] R. C. Thomson, J. P. Chick, and G. P. Harrison, "An LCA of the pelamis wave energy converter," *Int. J. Life Cycle Assessment*, vol. 24, no. 1, pp. 51–63, Jan. 2019.
[29] A. Poullikkas, "Technology prospects of wave power systems," *Electron. J. Energy Environ.*, vol. 2, no. 1, pp. 47–69, 2014.
[30] J. P. Kofoed, P. Frigaard, and M. Kramer, "Recent developments of wave energy utilization in Denmark," in *Proc. Workshop Renew. Ocean Energy Utilization: 20th Annu. Conf. Korean Soc. Ocean Eng.*, 2006, pp. 1–8.
[31] R. Yemm, D. Pizer, C. Retzler, and R. Henderson, "Pelamis: Experience from concept to connection," *Philos. Trans. Roy. Soc. A, Math., Phys. Eng. Sci.*, vol. 370, no. 1959, pp. 365–380, 2012.
[32] A. Weinstein, G. Fredrikson, M. J. Parks, and K. Nielsen, "AquaBuOY–the offshore wave energy converter numerical modeling and optimization," in *Proc. Oceans MTS/IEEE Techno-Ocean*, Kobe, Japan, vol. 4, Nov. 2004, pp. 1854–1859.
[33] D. Silva, E. Rusu, and C. Soares, "Evaluation of various technologies for wave energy conversion in the Portuguese nearshore," *Energies*, vol. 6, no. 3, pp. 1344–1364, Mar. 2013.
[34] A. Farkas, N. Degiuli, and I. Martić, "Assessment of offshore wave energy potential in the croatian part of the Adriatic sea and comparison with wind energy potential," *Energies*, vol. 12, no. 12, p. 2357, Jun. 2019.
[35] N. H. Samrat, N. B. Ahmad, I. A. Choudhury, and Z. Taha, "Prospect of wave energy in Malaysia," in *Proc. IEEE 8th Int. Power Eng. Optim. Conf. (PEOCO)*, Mar. 2014, pp. 127–132.
[36] N. A. M. Nasir and K. N. A. Maulud, "Wave power potential in Malaysian territorial waters," in *Proc. 8th IGRSM Int. Conf. Exhib. Geospatial Remote Sens. (IGRSM)*, Kuala Lumpur, Malaysia, vol. 37, Apr. 2016, pp. 1–9.
[37] E. P. Ciang, Z. A. Zainal, P. A. A. Narayana, and K. N. Seetharamu, "Potential of renewable wave and offshore wind energy sources in Malaysia," in *Proc. Int. Symp. Renew. Energy: Environ. Protection Energy Solution Sustain. Develop.*, Kuala Lumpur, Malaysia, 2003, pp. 1–11.
[38] M. Baba, "Wave power potential of Lakshadweep and Andaman and Nicobar Islands," *Indian J. Geo-Mar. Sci.*, vol. 17, no. 4, pp. 330–332, Dec. 1988.
[39] G. Kim, W. M. Jeong, K. S. Lee, K. Jun, and M. E. Lee, "Offshore and nearshore wave energy assessment around the Korean peninsula," *Energy*, vol. 36, no. 3, pp. 1460–1469, Mar. 2011.
[40] F. Sharkey, "Offshore electrical networks and grid integration of wave energy converter arrays-techno-economic optimisation of array electrical networks, power quality assessment, and Irish market perspectives," Ph.D. dissertation, Elect. Electron. Eng., Ocean Eng., Univ. Dublin, Dublin, Ireland, 2015.
[41] J. P. Sierra, C. Martín, C. Mösso, M. Mestres, and R. Jebbad, "Wave energy potential along the Atlantis coast of Morocco," *Renew. Energy*, vol. 96, pp. 20–32, Apr. 2016.
[42] N. Guillou and G. Chapalain, "Annual and seasonal variabilities in the performances of wave energy converters," *Energy*, vol. 165, pp. 812–823, Dec. 2018.
[43] V. Sanil Kumar and T. R. Anoop, "Wave energy resource assessment for the Indian shelf seas," *Renew. Energy*, vol. 76, pp. 212–219, Apr. 2015.
[44] Statista Research Department, *Electricity Generation Per Unit of Fuel Used United States*, Statista, Hamburg, Germany, 2016.
[45] D. C. Y. Foo. (2015). *The Malaysian Chemicals Industry: From Commodities to Manufacturing*. [Online]. Available: https://www.aiche.org/resources/publications/cep/2015/november/malaysian-chemicals-industry-commodities-manufacturing
[46] *Stationary Internal Combustion Sources*, vol. 1, 5th ed. United States Environmental Protection Agency, Washington, DC, USA, 2020, Ch. 3.
[47] Y. S. Lim and S. L. Koh, "Analytical assessments on the potential of harnessing tidal currents for electricity generation in Malaysia," *Renew. Energy*, vol. 35, no. 5, pp. 1024–1032, May 2010.
[48] A. H. Sharudin. (2021). *Gas Malaysia Lowers Average Natural Gas Selling Price to RM22.14/MMBtu for 1Q21*. [Online]. Available: https://www.theedgemarkets.com/article/gas-malaysia-lowers-average-selling-price-rm2214mmbtu-1q21#:~:text=KUALA%20LUMPUR%20(Jan%2012)%3A,1Q21)%2C%20which%20is%20RM11
[49] S. Barstow, G. Mørk, L. Lønseth, and J. P. Mathisen, "Worldwaves wave energy resource assessments from the deep ocean to the coast," in *Proc. 8th Eur. Wave Tidal Energy Conf.*, Uppsala, Sweden, 2009, pp. 1–11.
[50] L. Zhou, J. Li, C. Zheng, and X. Chen, "Wave energy research in global oceans with ERA-40 wave data for recent 45 years," in *Proc. Int. Conf. Remote Sens., Environ. Transp. Eng.*, Jun. 2011, pp. 3760–3763, doi: 10.1109/RSETE.2011.5965146.
[51] S. G. Shen and X. Z. Qian, *Resources Ocean–Develop and Utilize the Rich Blue Treasures*. Singapore: Haichao Press, 2003.
[52] A. Mirzaei, F. Tangang, and L. Juneng, "Wave energy potential assessment in the central and southern regions of the South China sea," *Renew. Energy*, vol. 80, pp. 454–470, Aug. 2015.

[53] C. Zheng, H. Zhuang, X. Li, and X. Li, "Wind energy and wave energy resources assessment in the East China Sea and South China Sea," *Sci. China Technol. Sci.*, vol. 55, no. 1, pp. 163–173, 2011.
[54] C. Zheng, C. Li, H. Wu, and M. Wang, *21st Century Maritime Silk Road: Construction of Remote Islands and Reefs*. Singapore: Springer, 2019.
[55] K. Sasmal, A. Webb, T. Waseda, and S. Miyajima, "Wave energy resource assessment: A comparative study for two coastal areas in Japan," in *Advances in Renewable Energies Offshore*. London, U.K.: Taylor & Francis Group, 2019.

ZAFARULLAH NIZAMANI received the bachelor's degree in civil engineering from Mehran University of Engineering and Technology, Pakistan, in 1991, the master's degree in structural engineering from NED University of Engineering and Technology, Pakistan, in 2002, and the Ph.D. degree in civil engineering (offshore structures) from Universiti Teknologi PETRONAS, Malaysia, in 2013.

Since 2013, he has been working with Universiti Tunku Abdul Rahman (UTAR), Malaysia. His current research interests include reliability of structures under various types of loads, such as metocean, fire and seismic, stochastic modeling, and wave-current interaction.

LEE LI NA received the bachelor's degree in environmental engineering from Universiti Tunku Abdul Rahman, in 2021.

AKIHIKO NAKAYAMA received the bachelor's degree in civil engineering from Japanese University, in 1970, and the master's and Ph.D. degrees in mechanics and hydraulics engineering from The University of Iowa, Iowa City, IA, USA.

Since 1990, he has been an Associate Professor with Kobe University, Japan. From 1997 to 2012, he was a Professor in civil engineering and environmental science. Since 2014, he has been teaching at the Department of Environmental Engineering, Univeristi Tunku Abdul Rahman, Kampar, Perak, Malaysia. He did his research at private industry, then McDonnell Douglas Corporation. His research interests include experimental fluids and hydraulic engineering, in 1980 and 1990, respectively, and numerical simulation and field survey of environmental hydraulics.

MONTASIR OSMAN AHMED ALI received the master's degree in structural engineering and the Ph.D. degree in civil engineering (offshore structures).

He is currently a Senior Lecturer with Universiti Teknologi PETRONAS (UTP). He is also heading the UTP Offshore Laboratory and managing the M.Sc. in offshore engineering programme at UTP. He specializes in hydrodynamics of floating offshore platforms and its station keeping systems, including numerical modeling and physical model testing. He is also looking into renewable energy, particularly hydrodynamic and aerodynamic stability of floating wind turbines. He provided several trainings on the hydrodynamics of offshore structures to the industry and academia. He spent more than seven years in structural engineering industry (contractor and consultancy companies) prior joining academia. He has published more than 30 articles in high reputational journals and conferences.

MUSHTAQ AHMED NIZAMANI received the B.E. degree in agriculture from SAU, Tando Jam, Pakistan. He is currently pursuing the master's degree in environmental engineering with University Tunku Abdul Rahman (UTAR), Perak, Malaysia. He is currently working as a Research Scholar with UTAR. His research interests include computational fluid dynamics (CFD), fluid flow analysis, load analysis on offshore structures, and water resource management.